Determination of (*n*,*k*) for absorbing thin films using reflectance measurements

J. M. Siqueiros, Luis E. Regalado and R. Machorro

We propose a method for determination of the complex refractive index of absorbing materials either in bulk or film geometry by measuring its reflectivity when coated with a well-characterized transparent dielectric at two specific optical thicknesses: $n_1d_1 = \lambda_0/4$ and $n_1d_1 = \lambda_0/2$. The complex refractive index of the sample $\tilde{n} = (n, k)$ is calculated for the monitoring wavelength λ_0. The selected optical thicknesses of the coating allow the calculation of its geometrical thickness, therefore the variation of $\tilde{n}$ with wavelength in the region where the reflectivity is measured can be determined.

I. Introduction

There are many methods for determination of the optical constants of thin films; several reviews were published before computers were developed and accessible to everybody.[1-3] Since then, many other methods have been proposed[4-12] using the advantages of accurate commercial apparatus for both, measurements and calculations. However, a comparison of several techniques and methods used in different laboratories for characterizing the same samples[13] shows considerable discrepancies among their results.

We present here our method for determining the complex refractive index of thin metal film samples. It is based on reflectance measurements that can be obtained in a conventional spectrophotometer or with a monitoring attachment in the evaporation chamber; the convenience of this method is the small effect that the experimental errors have on the determination of the thickness and (*n*,*k*) of the dielectric and that it provides comparable results with those obtained by more elaborate techniques.

A discussion is given for an absorbing thin film characterized in the visible spectral region and a comparison is made with results reported in the literature.

Luis Regalado is with Universidad de Sonora, Centro de Investigacion en Fisica, Apdo. Postal H-88, Hermosillo, Sonora, Mexico; the other authors are with Universidad Nacional Autonoma de Mexico, Instituto de Fisica, Lab. Ensenada, Apdo. Postal 2681, Ensenada, B.C., Mexico.

Received 23 March 1988.
0003-6935/88-204260-05$02.00/0.

II. Reflectance Data

Since we wish to determine a complex refractive index we must know at least two relevant experimental values; our choice is the reflectance (R), because it allows the study of opaque films as well as bulk materials, measured at two different conditions, which are defined as follows.

One part of the sample is coated with a transparent dielectric of optical thickness h, defined as the film thickness times the refractive index, equal to $\lambda_0/4$, and the other part with the same dielectric but optical thickness of $\lambda_0/2$ for a given wavelength λ_0, as shown in Fig. 1. In practice, this can be done in a single run of the evaporating plant, overcoating the absorbing layer with the selected dielectric of real index n_1, until the $\lambda_0/4$ optical thickness is reached. At this point, part of the sample is masked and the evaporation continues until the $\lambda_0/2$ thickness is obtained. The dielectric material should be well characterized, that is, $n_1(\lambda)$ must be known for the working spectral region.

At λ_0, usually known as the monitoring wavelength since it is used to control the thickness of the layer, the reflectance of the system is equal to that of the bare sample when the optical thickness of the overcoating is $\lambda_0/2$ while it takes a different value for $\lambda_0/4$, depending on the index.

The variation of the reflectance with overcoating thickness is shown in Fig. 2 and can be easily explained by the admittance method proposed by Macleod.[14] Figure 2(a) presents the reflectance variation of the sample as it is overcoated with the dielectric; Fig. 2(b) corresponds to the reflectance changes of a witness substrate. The coating thickness is optically controlled on a witness glass, placed near the sample in the vacuum chamber. The evaporation is suspended at the turning point of the R vs h curve.

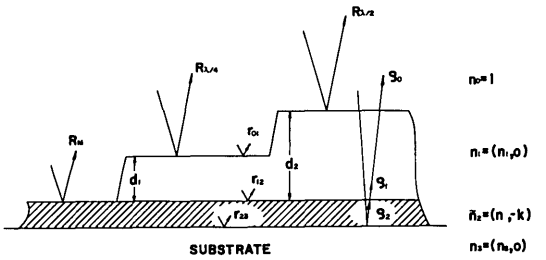

Fig. 1. System metal layer overcoated with a well-characterized dielectric film at two different thicknesses. The Fresnel reflectance coefficients are denoted by r_{ij}, depending on the interface (i,j), and the accumulated coefficient by ρ.

The selected optical thicknesses are shown in Fig. 3. The admittance of the substrate-absorbing layer system describes an almost circular locus, prescribed by their optical constants and the thickness of the layer. As the film becomes thicker, the locus approaches the bulk admittance y_b and, eventually, the properties of the metallic film predominate. The sample system may have any admittance Y between n_s and y_b, depending on the metal film thickness; this value of Y will be the starting point for admittance calculations of the overcoating.

Because the overcoating layer is a dielectric, the path is a circle with the center on the real axis. The location of the points corresponding to the $\lambda_0/4$ and $\lambda_0/2$ thicknesses is shown in Fig. 3. From the same figure it can be seen that they do not necessarily define the extrema values of R.

III. Determination of $\tilde{n} = (n,k)$

A. Calculations at λ_0

Analytically, selecting the thicknesses of the overcoatings, $h_1 = n_1 d_1$ as being a multiple of λ_0, represents a simplification in the use of thin-film formulation.

We use the recurrence formulation described by Dupoisot and Morizet,[15] which requires the calculation of a previous layer as input data for the next one, thus we need to calculate:

(a) the substrate to first layer reflection coefficient r_{02},

(b) the effect of propagation through the first layer, i.e., the sample,

(c) the reflection coefficient between layers 1 and 2, r_{12}, and

(d) the cumulative effect of the propagation of the electromagnetic field through the stack of layers.

Considering the geometry of the stack as the one shown in Fig. 1 and using the recurrence equation, we can write, for the reflection coefficient of the uncoated metal layer of thickness d_2 deposited on a glass substrate,

$$\rho_0 = [r_{02} + r_{23}\exp(-i2\delta_2)]/[1 + r_{02}r_{23}\exp(-i2\delta_2)], \qquad (1)$$

where $\delta_2 = (2\pi/\lambda_0)\tilde{n}_2 d_2$. For the metallic layer, overcoated with the transparent dielectric, the reflection coefficient is modified as follows:

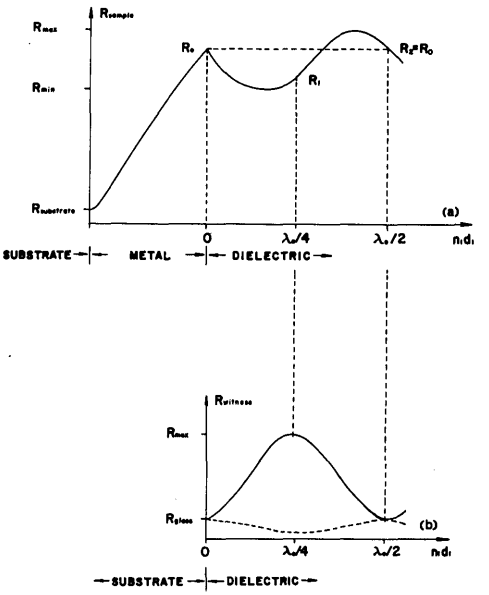

Fig. 2. Optical monitor signal, starting from the substrate, for the (a) metallic sample and (b) witness glass as a function of the thickness.

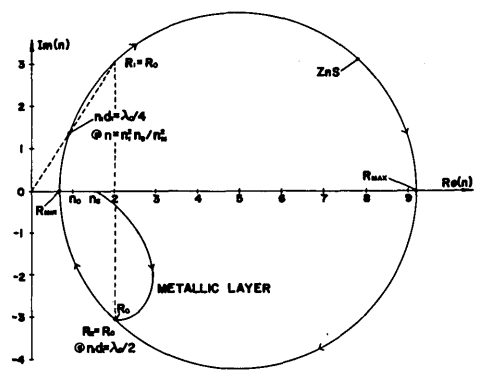

Fig. 3. Admittance loci for the glass substrate, metallic and dielectric layers system. The thicknesses are defined by the arc length of the circles, but this relation is not linear. The extrema of reflectance are located at the intersection of the circles with the real axis.[14]

$$\rho_0 = [r_{01} + \rho_1\exp(-i2\delta_1)]/[1 + r_{01}\rho_2\exp(-i2\delta_1)], \qquad (2)$$

where $\rho_1 = [r_{12} + \rho_2\exp(-i2\delta_m)]/[1 + r_{12}\rho_2\exp(-i2\delta_m)]$, $\rho_2 = r_{23}$,

ρ_1 is the partial reflection from both interfaces of the sample, and

$\delta_1 = (2\pi/\lambda_0)n_1 d_1$ is the phase thickness of the overcoating.

Let us simplify the equation for ρ_0 for our particular situation of interest. When $n_1 d_1 = \lambda_0/4$, $\delta_1 = \pi/2$, and $\exp(-i2\delta_1) = -1$, reducing ρ_0 to $\rho_0 = (r_{01} - \rho_2)/(1 - r_{01}\rho_2)$, which can be rewritten as

$$\rho_0 = \frac{[r_{01} - r_{12} + (r_{01}r_{12} - 1)r_{23}\exp(-i2\delta_1)]}{[1 - r_{01}r_2 + (r_{12} - r_{01})r_{23}\exp(-i2\delta_1)]}. \qquad (3)$$

When $n_1 d_1 = \lambda_0/2$, $\delta_1 = \pi$, and $\exp(-i2\delta_1) = 1$, so $\rho_0 = (r_{01} + \rho_1)/(1 + r_{01}\rho_1)$, and this equation must be equal to Eq. (1) at λ_0 only. Indeed, for the given wavelength,

the coating film acts as an absentee layer. In this case, $r_{01} = r_{23}$ and Eq. (2) becomes

$$\rho_0 = [r_{02} + r_{23}\exp(-i2\delta_1)]/[1 + r_{02}r_{23}\exp(-i2\delta_1)]. \quad (4)$$

Equations (3) and (4) are used for calculating the corresponding reflectance values. The resulting reflectance expressions may then be solved for n and k at the monitoring wavelength λ_0; the solution requires the knowledge of $n_1(\lambda_0)$ and the sample thickness d_2. The latter must be measured by an alternative technique, such as interference microscopy[16] or ellipsometry.[17]

A special case is when the sample is opaque, that is, when the Fresnel coefficient at the second interface may be neglected, $r_{23} = 0$. Equations (3) and (4) become independent of δ_1, and we can make

$$R_{(\lambda/4)} = [(r_{01} - r_{12})/(1 - r_{01}r_{12})]^2,$$
$$R_{(\lambda/2)} = [r_{02}]^2,$$

from which we can easily determine

$$n = (n_1^4 - 1)/[2(n_1^2 R^*_{\lambda/4} - R^*_{\lambda/2})], \quad (5)$$

$$k^2 = 2 \cdot n \cdot (R^*_{\lambda/2}) - (n^2 + 1), \quad (6)$$

where $R^*(\lambda/j) = (1 + R_j)/(1 - R_j)$, with $j = 2,4$. Subscript 4 corresponds to a quarterwave (QW) and subscript 2 to a halfwave (HW). We are assuming air as incident medium $n_0 = 1$.

B. Calculation of $\tilde{n}$ for any Wavelength

To extend the previous results to the most general situation, first we calculate the overlayer geometrical thickness for $\lambda = \lambda_0$ for the two regions. The one coated with QW has a physical thickness of $d_1 = \lambda_0/[4n_1(\lambda_0)]$, and the region with a HW coating has $d_1 = \lambda_0/[2n_1(\lambda_0)]$. For $\lambda = \lambda_0$, δ_1 is no longer a multiple of $\pi/2$ but has new values:

$$\delta_1 = (\pi/2)[n_1(\lambda)/n_1(\lambda_0)](\lambda_0/\lambda) \quad \text{for QW},$$
$$\delta_1 = (\pi)[n_1(\lambda)/n_1(\lambda_0)](\lambda_0/\lambda) \quad \text{for HW}.$$

These values may be substituted in Eq. (2), giving two new equations from which we have to numerically determine $n(\lambda)$ and $k(\lambda)$.

The zeros of the general equations obtained from Eq. (2) are simultaneously solved for n and k using Newton's method where the derivatives are calculated numerically using Pachner's algorithm.[18]

IV. Results

The results of the application of this method are presented below, with the corresponding uncertainties produced by induced experimental errors. To verify the reproducibility and confidence of these results, we simulate an experiment. Using reported data for some metals, we calculate its reflectance as a function of wavelength when they are overcoated with a dielectric film, zinc sulfide in our case. Using the calculated reflectance R for two different thicknesses as experimental data, our aim is to recover the metal optical properties.

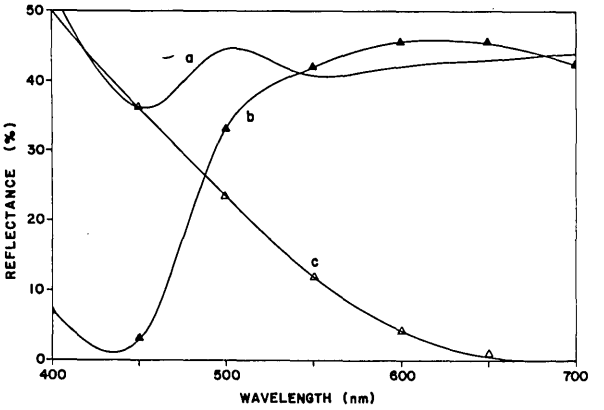

Fig. 4. Experimental reflectance for Rh thin film over glass substrate (curve a), calculated using data taken from Ref. 13; the same metal is overcoated with a dielectric of optical thickness of $\lambda_0/2$ (curve b) and $\lambda_0/4$ (curve c).

As an example, we used the data for rhodium, reported by Arndt *et al.*[13] First we took the average of the refractive-index values obtained by different techniques for a 15.5-nm Rh film (Fig. 4, curve a). Then we simulated a coating with ZnS, Fig. 4, curve b for HW and Fig. 4, curve c for QW. The dielectric thickness was monitored in a witness glass giving a reflectance maximum at $n_1d_1 = \lambda_0/4$ and at $n_1d_1 = \lambda_0/2$, the bare Rh film reflectance, according to Fig. 2(b). The reflectances of the sample are taken as our experimental values from which we determine the solutions for $n(\lambda)$ and $k(\lambda)$ starting at λ_0.

In a real experiment there are several error sources, e.g., uncertainties in thickness and reflectance measurements, which affect the final result. To simulate these effects we use the Monte Carlo technique, assuming the uncertainties have a Gaussian distribution. The input values of the reflectance of the sample, at two different overcoating thicknesses, are displaced from the ideal figures according to the standard deviation introduced for this parameter. The same procedure is applied to the thickness of the metallic sample and overcoating. The value of the standard deviation to be used depends on the technique and care used to make the measurements. A set of fifty runs was made taking random values, with the Gaussian distribution centered at the ideal figures. At this point we performed a most important sampling by chopping the Gaussian tails off at 1.5 times the standard deviation. The distribution of the mean value of (n,k) and its standard deviation reflect the capability of the method to recover the optical properties from reflectance measurements.

Figure 5 is a summary of our results. Starting with the ideal situation, where all the measurements are perfectly made, the reflectance and thickness uncertainties $\sigma_R, \sigma_{d1}, \sigma_{d2}$, respectively, are zero. We found that for the fifty runs $\sigma_n = \sigma_k = 0$, the index determination is also perfect.

For the sake of clarity we include tables associated with each figure with average values and its standard

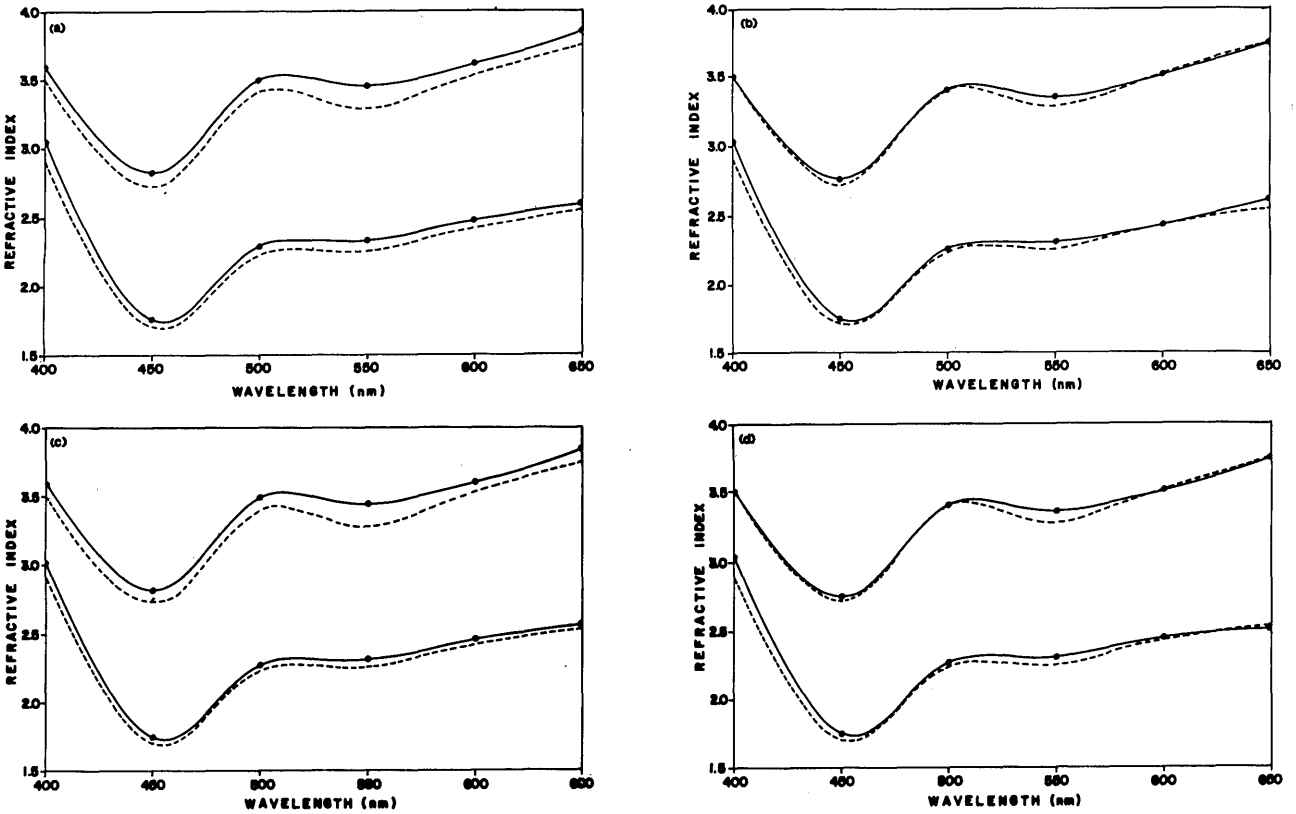

Fig. 5. Complex refractive index of the Rh as a function of wavelength, obtained using the method described in the text. Upper set of curves are the imaginary part of the index, lower set the real part. Expected values are plotted with broken line. The standard deviations corresponding to certain experimental errors are presented in the associated tables. (a) Table I, (b) Table II, (c) Table III, (d) Table IV.

deviation for fifty sample measurements (Tables I, II, III, and IV).

The most sensitive parameter is the dielectric thickness, a variation of 5 nm (~8%) introduces an error of 15%, assuming the two other parameters are perfectly defined [Fig. 5(a)].

The imaginary part of the complex refractive index depends strongly on the thickness accuracy. If only the reflectance has errors, both $\mathrm{Re}(\tilde{n})$ and $\mathrm{Im}(\tilde{n})$ are fairly well reproduced [Fig. 5(b)]. If the σ_d is larger, the imaginary part loses accuracy very quickly, as can be seen in Figs. 5(c) and (d).

Table I. Average Values and Standard Deviation (Fig. 5(a))

$\sigma_R = 0.0\%$	$\sigma_{d2} = 0$ nm		$\sigma_{d1} = 5$ nm	
Wavelength	$\mathrm{Re}(\tilde{n})$		$\mathrm{Im}(\tilde{n})$	
(nm)	n	σ_n	k	σ_k
400	3.060	0.112	3.603	0.590
450	1.760	0.0366	2.824	0.452
500	2.291	0.0287	3.496	0.541
550	2.334	0.0470	3.449	0.549
600	2.473	0.0730	3.611	0.576
650	2.598	0.0945	3.842	0.606

Table II. Average Values and Standard Deviation (Fig. 5(b))

$\sigma_R = 0.4\%$	$\sigma_{d2} = 0$		$\sigma_{d1} = 0$	
Wavelength	$\mathrm{Re}(\tilde{n})$		$\mathrm{Im}(\tilde{n})$	
(nm)	n	σ_n	k	σ_k
400	3.035	0.0639	3.515	0.0317
450	1.750	0.0447	2.760	0.0596
500	2.263	0.0267	3.409	0.0214
550	2.306	0.0368	3.357	0.0236
600	2.436	0.0482	3.519	0.0278
650	2.614	0.127	3.751	0.0289

Table III. Average Values Standard Deviation (Fig. 5(c))

$\sigma_R = 0.0\%$	$\sigma_{d2} = 3$ nm		$\sigma_{d1} = 3$ nm	
Wavelength	$\mathrm{Re}(\tilde{n})$		$\mathrm{Im}(\tilde{n})$	
(nm)	n	σ_n	k	σ_k
400	3.021	0.0607	3.597	0.317
450	1.744	0.0205	2.815	0.247
500	2.272	0.0097	3.487	0.295
550	2.318	0.0193	3.441	0.299
600	2.457	0.0346	3.603	0.315
650	2.582	0.0468	3.833	0.331

Table IV. Average Values and Standard Deviation (Fig. 5(d))

$\sigma_R = 0.4\%$	$\sigma_{d2} = 3$ nm		$\sigma_{d1} = 3$ nm	
Wavelength	$\mathrm{Re}(\tilde{n})$		$\mathrm{Im}(\tilde{n})$	
(nm)	n	σ_n	k	σ_k
400	3.047	0.0994	3.515	0.305
450	1.749	0.0419	2.745	0.258
500	2.271	0.0302	3.416	0.283
550	2.309	0.0340	3.366	0.289
600	2.446	0.0642	3.522	0.305
650	2.512	0.139	3.745	0.325

V. Conclusion

We present a method based on reflectance measurements for the determination of the complex refractive index of an absorbing thin film. The experimental data and its possible deviations suggest that our method may be accurate even in the presence of experimental errors. We show that by properly selecting the thickness of the dielectric overcoating it is possible to obtain the optical properties of a metallic film.

This work was partially done at INAOE, Puebla, for which two of the authors (R.M. and L.E.R.) are grateful. L.E.R. wishes to thank DIGSA-SEP for its economic support.

References

1. F. Abeles, "Methods for Determining Optical Parameters of Thin Films," Prog. Opt. **2**, 249 (1963).
2. O. S. Heavens, "Measurement of Optical Constants of Thin Films," Phys. Thin Films **2**, 193 (1964).
3. P. Rouard and P. Bousquet, "Optical Constants of Thin Films," Prog. Opt. **4**, 145 (1965).
4. J. M. Bennett and M. J. Booty, "Computational Method for Determining n and k for a Thin Film from the Measured Reflectance, Transmittance, and Film Thickness," Appl. Opt. **5**, 41 (1966).
5. C. L. Nagendra and G. K. M. Thutupalli, "Determination of Optical Properties of Absorbing Materials: a Generalized Scheme," Appl. Opt. **22**, 587 (1983).
6. S. G. Tomlin, "More Formulae to Optical Reflection and Transmission by Thin Films," J. Phys. D **5**, 847 (1972).
7. J. P. Borgogno, B. Lazarides, and E. Pelletier, "Automatic Determination of the Optical Constants of Inhomogeneous Thin Films," Appl. Opt. **21**, 4020 (1982).
8. J. E. Nestell, Jr., and R. W. Christy, "Derivation of Optical Constants of Metals from Thin-Film Measurements at Oblique Incidence," App. Opt. **11**, 643 (1972).
9. J. C. Manifacier, J. Gasiot, and J. D. Fillard, "A Simple Method for the Determination of the Optical Constants, n,k and the Thickness of a Weakly Absorbing Thin Film," J. Phys. E **9**, 1002 (1976).
10. W. E. Case, "Algebraic Method for Extracting Thin-Film Optical Parameters from Spectrophotometer Measurements," Appl. Opt. **22**, 1832 (1983).
11. J. A. Dobrowolski, F. C. Ho, and A. Waldorf, "Determination of Optical Constants of Thin Film Coating Materials Based on Inverse Synthesis," Appl. Opt. **22**, 3191 (1983).
12. E. Elizalde, "On the Determination of the Optical Constants $n(\lambda)$ and $k(\lambda)$ of Thin Supported Films," Thin Solid Films **122**, 45 (1984).
13. D. P. Arndt *et al.*, "Multiple Determination of the Optical Constants of Thin-Film Coating Materials," Appl. Opt. **23**, 3571 (1984).
14. H. A. Macleod, *Thin-Film Optical Filters* (Adam Hilger, Bristol, 1986).
15. H. Dupoisot and J. Morizet, "Thin Film Coatings: Algorithms for the Determination of Reflectance and Transmittance, and Their Derivatives," Appl. Opt. **18**, 2701 (1979).
16. S. Tolansky, *Multiple-Beam Interferometry of Surfaces and Films* (Clarendon, Oxford, 1983).
17. R. M. Azzam and N. M. Bashara, *Ellipsometry and Polarized Light* (North-Holland, New York, 1977).
18. J. Pachner, *Handbook of Numerical Analysis Applications* (McGraw-Hill, New York, 1984).

NASA *continued from page 4199*

The time-of-flight mass spectrometer sends out a trigger pulse at the beginning of each cycle. The microchannel-plate detector of the spectrometer produces an ac component containing the spectral signal, and a dc component—the total multiplier current—that is a measure of all the masses in the vapor. The spectral signals are fed to a transient recorder (synchronized by the trigger pulses from the spectrometer) where they are stored in a signal memory and processed by a microprocessor before being transferred to the host computer.

This work as done by K. A. Lincoln of Ames Research Center and R. D. Bechtel of Santa Clara University. Further information may be found in NASA TM-88374 [N88-724538/NSP], "A Fast Data Acquisition System for the Study of Transient Events by High Repetition Rate Time-of-Flight Mass Spectrometer." Copies may be purchased [prepayment required] from the National Technical Information Service, Springfield, VA 22161. Inquiries concerning rights for the commercial use of this invention should be addressed to the Patent Counsel, Ames Research Center Attn: D. G. Brekke, Mail Code 200-11, Moffett Field, CA 94035. Refer to ARC-11785.

Reliability of inspection by scanning laser acoustic microscopy

A report describes an evaluation of scanning laser acoustic microscopy (SLAM) in the detection of surface voids in silicon nitride and silicon carbide. SLAM is an attractive technique for the nondestructive inspection of these ceramics because it can image surface and subsurface microflaws in real time. The detection of such flaws is important because they limit the strengths and fracture toughnesses of ceramic parts in advanced high-temperature heat engines. In SLAM, a laser light is used to detect distortions, on an angstrom scale, produced on the surface of a specimen by ultrasonic waves transmitted through the specimen. From the distortion, SLAM creates a picture on a video monitor of such defects as voids, inclusions, and cracks.

In the evaluation, specimens of sintered Si_3B_4, and SiC were examined by SLAM at an ultrasonic frequency of 100 MHz, in both the as-fired condition and after polishing. The specimens were intentionally impressed with styrene microspheres during firing to introduce voids of known size, shape, number, and location in the surface. The evaluation concentrated on the statistical reliability of the detection of voids by SLAM. In the polished specimens, SLAM detected surface voids as small as 100 μm in diameter with 0.90 probability at a confidence level of 0.95. However, the reliability of detection was substantially less for voids in unpolished as-fired specimens. Moreover, inspection of the as-fired specimens took ten times as long as the inspection of the smooth specimens. If ceramic engine parts are smoothly finished, as they are likely to be, the SLAM technique should detect surface and near-surface flaws quickly and reliably.

This work was done by Don J. Roth, Stanley J. Klima, and James D. Kiser of Lewis Research Center and George Y. Baakini of Cleveland State University. Further information may be found in NASA TM-87035[N85-32337/NSP], "Reliability of Void Detection in Structural Ceramics Using Scanning Laser Acoustic Microscopy." Copies may be purchased [prepayment required] from the National Technical Information Service, Springfield, VA 22161, Telephone No. (703) 487-4560. Rush orders may be placed for an extra fee by calling (800) 336-4700. Refer to LEW-14633.

continued on page 4273